# Integrated Resource Management for Terrestrial-Satellite Systems

Shu Fu ⬢, Jie Gao ⬢, *Member, IEEE*, and Lian Zhao ⬢, *Senior Member, IEEE*

*Abstract*—As data traffic in terrestrial-satellite systems surges, the integration of power allocation for caching, computing, and communication (3C) has attracted much research attention. However, previous works on 3C power allocation in terrestrial-satellite systems mostly focus on maximizing the overall system throughput. In this paper, we aim to guarantee both throughput fairness and data security in terrestrial-satellite systems. Specifically, we first divide the system implementation into three steps, i.e., data accumulation, blockchain computing, and wireless transmission. Then, we model and analyze the delay and power consumption in each step by proposing several theorems and lemmas regarding 3C power allocation. Based on the theorems and lemmas, we further formulate the problem of 3C power allocation as a Nash bargaining game and construct an optimization model for the game. Last, we solve the optimization problem using dual decomposition and obtain the optimal period of the satellite serving the ground stations as well as the optimal 3C power allocation solution. The optimal solution can provide guidelines for parameter configuration in terrestrial-satellite systems. The performance of the proposed terrestrial-satellite architecture is verified by extensive simulations.

*Index Terms*—Nash bargaining game, fairness, security, 3C, resource management, terrestrial-satellite systems.

## I. INTRODUCTION

**T**ERRESTRIAL-SATELLITE systems [1]–[5] enable seamless coverage for ground users in a wide area [6]. This makes it very promising in the next generation of networks, especially in the scenarios of Internet of Things (IoT) and vehicle network, etc. Existing research on the performance of terrestrial-satellite systems has mostly focused on improving throughput [7], [8] by relatively fixed allocation of caching, computing, and communication resources.

S. Fu is with the College of Microelectronics and Communication Engineering, Chongqing University, Chongqing 400044, China, and also with the Chongqing Key Laboratory of Space Information Network and Intelligent Information Fusion, Chongqing University, Chongqing 400044, China (e-mail: shufu@cqu.edu.cn).

J. Gao is with the Department of Electrical and Computer Engineering, University of Waterloo, Waterloo, ON N2L 3G1, Canada (e-mail: jie.gao@uwaterloo.ca).

L. Zhao is with the Department of Electrical, Computer, and Biomedical Engineering, Ryerson University, Toronto, ON M5B 2K3, Canada (e-mail: l5zhao@ryerson.ca).

Digital Object Identifier 10.1109/TVT.2020.2964659

However, from the perspective of enhancing user experience in terrestrial-satellite systems, fairness [9]–[11] and security [12]–[18] are two critical issues that should not be overlooked. Especially, 3C (caching, computing [19], [20], and communication [21]) resource allocation involved in terrestrial-satellite systems providing fair and secure services is a hot topic effecting system performance.

Several existing works [9]–[11] have employed Nash bargaining game to provide user throughput fairness in wireless networks. Gao *et al.* consider user fairness based on Nash bargaining in a multiuser resource allocation game [9], where users with different quality of service (QoS) requirements achieve different throughput. This can effectively motivate users to cooperate to obtain a fair and improved network service for all. Ni *et al.* provide the joint channel and power allocation optimization in a wireless network based on Nash bargaining game [10]. Zhang *et al.* further consider imperfect wireless channel state information in a Nash bargaining game [11]. Bairagi *et al.* solve the issue of coexistence between two wireless systems based on a Nash bargaining game [22]. Xu *et al.* employ Nash bargaining to guarantee user fairness in mobile social networks [23]. These works focus on the performance of system throughput with fairness awareness. The impact of 3C resource management on the system performance is not considered.

In terms of data security in wireless systems, blockchain [12], [13], [15]–[17], [24] has attracted extensive attentions from both the academia and the industry. Tschorsch *et al.* introduce the development history of blockchain [24]. Fu *et al.* employ blockchain to guarantee data security in IoT [14]. Although 3C resource allocation and blockchain based data caching are studied in [14] to guarantee data security, integrated terrestrial-satellite system is not considered. Yang *et al.* propose a trust management mechanism for vehicular networks based on blockchain [12]. However, the above works focus on the blockchain based security mechanism, where the impact of 3C resource management on the blockchain based integrated terrestrial-satellite system is not considered.

Although many existing works have contributed to user fairness and data security in wireless systems, power allocation for each of the 3C is generally studied separately. However, for terrestrial-satellite systems, such separate 3C power allocation may lead to low resource utility decreasing the performance, considering the long distance between ground stations and satellites.

Motivated by the above observation, we propose a novel terrestrial-satellite network architecture with fairness and

security awareness, and formulate a joint optimization of satellite serving period and 3C power allocation in this paper. Specifically, we first formulate a terrestrial-satellite model, where low earth orbit (LEO) satellites will collect traffic data from ground stations periodically. In this paper, one period of the satellite serving the ground stations may contain multiple LEO satellite period around the earth.

Then, we divide the system implementation into three steps: traffic accumulation, computing, and wireless transmission, corresponding to caching, computing, and communication in 3C, respectively. In the traffic accumulation step, data is collected and accumulated as one data block. In the computing step, the ground station will continually calculate the hash value of the block with a random variable called "nonce". When the hash value is smaller than a threshold, the block can be reported to the LEO satellite in the wireless transmission step and added to the blockchain. We study the relationship between the delay in the three steps and the power consumption of 3C. Moreover, we can formulate the overall system power consumption under a maximal power constraint. Under the maximal power constraint, the period of the satellites serving the ground stations and the 3C power consumption will be jointly optimized.

Furthermore, we formulate the Nash bargaining framework for the considered terrestrial-satellite system. In the proposed model, Nash bargaining game guarantees fairness in the 3C power allocation. We demonstrate the existence and uniqueness of the Nash bargaining solution in the formulated game to find the bargaining solution using dual decomposition.

Our contributions can be summarized as follows:

- We reveal the relationship between the power consumption of 3C and the corresponding delay in the terrestrial-satellite system. We study that how the power allocation of 3C effects each other, considering fairness and security in the system. We provide several theorems and lemmas on 3C power allocation to explore the insights in optimizing the system performance.
- We propose a novel terrestrial-satellite architecture with fairness and security awareness. We formulate a Nash bargaining framework based optimization model for the considered terrestrial-satellite system.
- We obtain the optimal period of the satellites serving the ground stations and the optimal 3C power allocation. The solution provides guidelines for both the engineering implementation and the theoretical analysis of a fair and secure terrestrial-satellite system.

It is notably that besides fairness and security in an integrated terrestrial-satellite system, several other system performance evaluation criteria [25]–[28] should also be considered such as placement of controllers and gateways [25], service offloading [28], etc. In this paper, we do not consider these criteria due to the limited space, which will be considered in our future work. On the other hand, although the solving methods used in this work have been used in several existing works, such as the methods solving bargain game in [10], [11], the optimization problem considered in this work is totally different with the existing works.
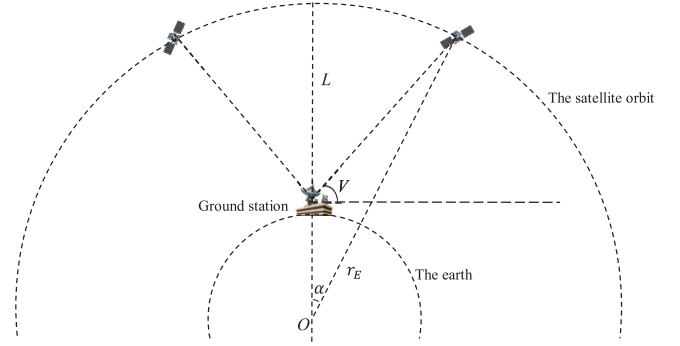


Fig. 1.　LEO satellite orbit model.

The remainder of this paper is organized as follows. Section II presents the system model and the problem formulation. Section III solves the considered model by dual decomposition. Numerical results demonstrate the performance of the proposed architecture and solution in terms of user fairness and data security in Section IV. We conclude the paper in Section V.

## II. SYSTEM MODEL AND PROBLEM FORMULATION

### A. LEO Satellite Orbit Model

The LEO satellite orbit is shown in Fig. 1. The circular orbit is assumed in this paper. $N$ ground stations are located at ground, which are served by the same satellite. Denote the radius of earth by $r_E$. We assume that the distance between the satellite and all ground stations is identical and equal to $L$. Similarly, the minimal elevation angle $V$ and the geocentric angle $\alpha$ from any ground station to the satellite are also identical. Then, it can be shown that $\alpha$ is

$$\alpha = \arccos\left(\frac{r_E}{L + r_E}\cos V\right) - V. \tag{1}$$

In Fig. 1, the satellite can serve the ground station continuously up to $2\alpha$ range of the geocentric angle. According to the Kepler's second law, the orbital period of the satellite around the earth, $T^{\text{LEO}}$, is

$$T^{\text{LEO}} = 2\pi\sqrt{\frac{(L + r_E)^3}{\mu}}, \tag{2}$$

where $\mu = 398,601.58 \text{ km}^3/\text{s}^2$ is the Kepler constant. Then, the available continuous serving time, referred to as *the time window*, of the satellite in each orbital period is

$$\widetilde{T} = \frac{2\alpha}{2\pi}T^{\text{LEO}}$$

$$= 2\left(\arccos\left(\frac{r_E}{L + r_E}\cos V\right) - V\right)\sqrt{\frac{(L + r_E)^3}{\mu}}. \tag{3}$$

In practice, each ground station connects to multiple data gathering devices. The data gathering devices accumulate traffic data and send the data to the ground station, which plays the role of as the data gateway. After data processing, the ground station transmits the data to its serving satellite in its time window
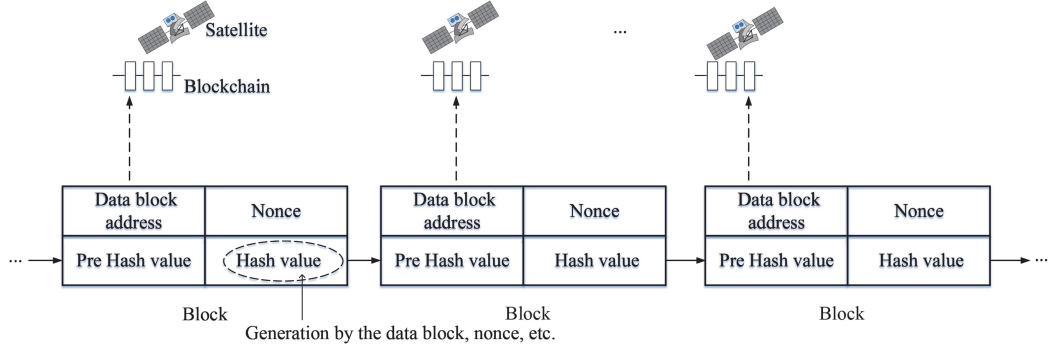
Fig. 2.    The connection of blocks in the blockchain.

periodically. In this paper, one serving period of the satellite can be a multiple of its orbital periods, i.e. $T^{\text{LEO}}$. Moreover, the satellite can serve at most one of the $N$ ground stations in each orbital period. On average, each ground station is served in an orbital period with a certain probability. We will discuss this in details in Sub-section II-B.

### B.  Blockchain Model

Blockchain can effectively enhance data security in a network. The user data can be stored and relayed in the satellite network to meet the traffic demand across the network. Take IoT data as one instance: the categories of IoT companies include the raw material acquisition, manufacturing process, production transportation, and production transactions. The IoT data generated by each company is gathered by the ground station serving the company and sent to the corresponding satellite. Thereafter, the data will be recorded into the blockchain at each satellite to guarantee the data security [14] in the satellite network.

The structure of the blockchain is shown in Fig. 2. Each block contains the caching address of the data block, a hash value, a nonce, and a hash value in the previous block. In practice, the block data may be stored and relayed in different satellites. The blockchain contains only the caching address of the data block instead of the whole data block itself. However, the generation of the hash value is still based on the data block, the nonce, and the hash value in the previous block. Note that satellite relay can be used when a ground station is out of the coverage area of a LEO satellite. However, this is beyond the scope of this paper, and we may study this in our future works.

3C in the blockchain is shown in Fig. 3. The ground station contains data loading cache for accumulating the block data. The computing servers are employed for blockchain computing, where the larger capacity of the computing servers can lead to the lower computing delay. The block is generated by the correct nonce, based on which the hash value should meet the hash threshold. Then, the block will be cached in the data transmission cache for wireless transmission when the satellite serves the ground station. The cache resource is limited by the wireless transmission capacity that we will discussed later, the computing resource is limited by the demand of blockchain computing, and the wireless transmission power is limited by the LEO satellite orbit as in Section II-A.
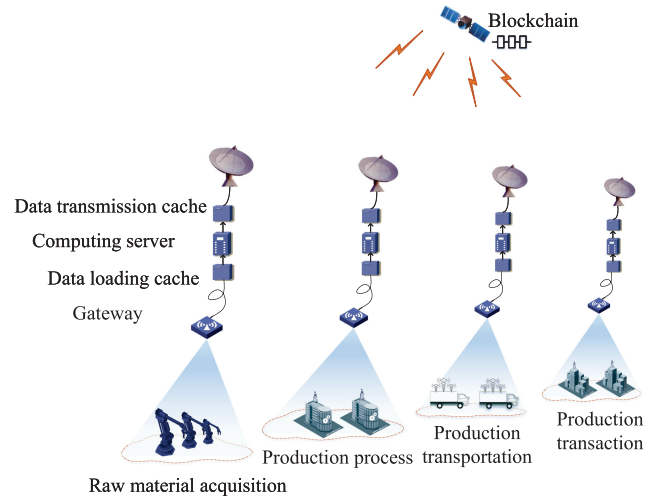


Fig. 3.    The proposed terrestrial-satellite architecture and the 3C in it.
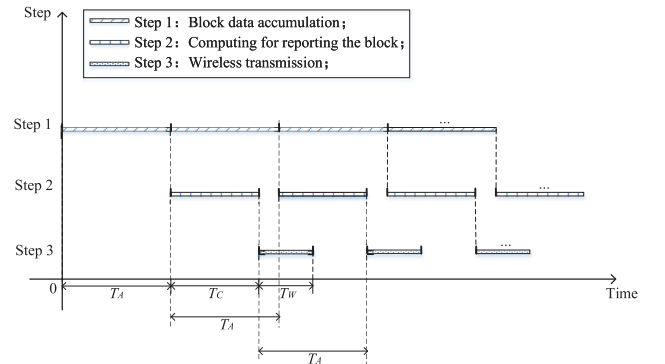


Fig. 4.    System steps.

The three system steps can be described as in Fig. 4. For ground station $i$, the system steps can consist of the traffic accumulation with $T_i^A$ seconds, blockchain computing with $T_i^C$ seconds, and the wireless transmission with $T_i^W$ seconds. In order to avoid data overflow in the cache, we have $T_i^C \leq T_i^A$ and $T_i^W \leq T_i^A$. Since the wireless transmission must be in the time window, we have $T_i^W \leq \widetilde{T} \leq T_i^A$, considering that a transmission service can happen every several orbital periods. Obviously, the three steps have the same period $T_i^A$.

In terms of caching in the 3C [29]–[34], the data loading cache is used to store the traffic data at the ground station. The demanded capacity of caches in the three steps should be the same as the length of the block for wireless transmission. We assume that the wireless channel bandwidth of the ground station is $B$ Hz, where the Gaussian white noise power is $\sigma^2$ watt (W). Assume that the wireless channel gain from the ground station $i$ to the satellite is $|h_i|^2$, and the wireless transmission power of the ground station is $P_i^W$. Then, the transmission rate of the ground station $i$, $R_i$, is

$$R_i = B \log_2 \left( 1 + \frac{P_i^W |h_i|^2}{\sigma^2} \right), \qquad (4)$$

and the length of the block sent in the transmission time $T_i^W$ is $R_i T_i^W$. The implementation of data processing is continuous and circulatory. After the data is accumulated to $R_i T_i^W$ bits in the data loading cache, the data will be cached in the computing server for generating the block. Finally, the block will be cached in the data transmission cache for wireless transmission as in Fig. 3.

In practice, the amount of cache in usage can be configured based on the maximal length of the data block. We denote the power consumption of caching by $P_S$ W/bit, and the maximal average power consumption at each ground station by $P_{\max}$. We know that the maximal continuous wireless serving time of the ground stations is $\widetilde{T}$. Then, the size of the required cache is the same in the three steps in Fig. 4. We introduce Lemma 1 to derive the length of cache.

*Lemma 1:* The maximal length of cache per step configured at the $i$-th ground station is

$$K_i = \widetilde{T} B \log_2 \left( 1 + \frac{P_{\max} T^{\mathrm{LEO}} |h_i|^2}{\widetilde{T} \sigma^2} \right).$$

*Proof:* With the maximal average power $P_{\max}$ during $T_i^A$, the maximal length of the cache per step in Fig. 4 can be determined by the case of maximizing the average user throughput:

$$\overline{R}_i = \frac{B T_i^W}{T_i^A} \log_2 \left( 1 + \frac{P_{\max} T_i^A |h_i|^2}{T_i^W \sigma^2} \right),$$

where $T^{\mathrm{LEO}} \le T_i^A$ and $T_i^W \le \widetilde{T}$. Next, we optimize $T_i^A$ and $T_i^W$ to obtain the upper bound of $\overline{R}_i$. It can be proved that $\overline{R}_i$ is monotonously decreasing with $T_i^A$, and thus we have $T_i^A = T^{\mathrm{LEO}}$ for maximizing $\overline{R}_i$. Likewise, we can further prove that $\overline{R}_i$ is monotonously increasing with $T_i^W$, then, we can have $T_i^W = \widetilde{T}$ for maximizing $\overline{R}_i$. Therefore, the length of the cache per step configured at the $i$-th ground station is

$$K_i = \widetilde{T} B \log_2 \left( 1 + \frac{P_{\max} T^{\mathrm{LEO}} |h_i|^2}{\widetilde{T} \sigma^2} \right).$$

In the above equation, $P_{\max} T^{\mathrm{LEO}}$ is the total energy consumption in one orbital period, and thus $P_{\max} T^{\mathrm{LEO}}/\widetilde{T}$ is the upper bound of power consumption for wireless transmission in $\widetilde{T}$. This equation indicates the upper bound of cache in each step, because that $P_{\max}$ is used for caching, computing, as well as communication, other than only for caching. ∎

Based on Lemma 1, the overall power consumption of the cache in the ground station $i$ is

$$\overline{P}_i^S = 3 P_S K_i = 3 P_S \widetilde{T} B \log_2 \left( 1 + \frac{P_{\max} T^{\mathrm{LEO}} |h_i|^2}{\widetilde{T} \sigma^2} \right). \qquad (5)$$

In practice, $\overline{P}_i^S$ is the upper bound of the caching power consumption. In this paper, the cache with capacity $3K_i$ is configured to rapidly caching the traffic data as an simplification in the system model. This approximation is based on the low cost of cache resource in practice. The caching power consumption based on the real-time cached data size and queuing theory will be studied in our future work.

In terms of computing in the 3C [35]–[37], the computing delay for generating the correct nonce to report the block is $T_i^C$. The variable nonce is generally found from a mathematical problem, and its value can be changed iteratively [12]. When the hash value of the block and the nonce value is below the pre-determined hash threshold, the block in the computing server can be transmitted to the satellite by the ground station. We define the threshold of the hash value by $M_0$ for each ground station, and the computing capacity of the $i$-th ground station by $C_i$ cycles per second (cps). Obviously, the hash value $M$ for generating and transmitting the block to the satellite should meet $M \le M_0$. This leads to the fair opportunity of generating the correct nonce with the same hash algorithm in each ground station. In this paper, we assume that the average number of iterations to generate the correct nonce meeting $M \le M_0$ is the same in each ground station and denoted by $\omega$. We denote the average number of CPU cycles in the computing server demanded for solving the hash function at a time by $C_H$ cycles. Then, $T_i^C$ meets

$$T_i^C = \frac{\omega C_H}{C_i}. \qquad (6)$$

Considering that $T_i^C \le T_i^A$, we have

$$C_i \ge \frac{\omega C_H}{T_i^A}. \qquad (7)$$

In terms of communication in the 3C, we focus on the wireless transmission of the ground stations in this paper. As in eq. (4), the transmission rate of the ground station $i$ is $R_i$ in the transmission time $T_i^W$ per period of the transmission $T_i^A$. This indicates that the average power consumption of the wireless transmission is

$$\overline{P}_i^W = \frac{P_i^W T_i^W}{T_i^A}, \qquad (8)$$

where the period of the wireless transmission (*i.e.*, serving period) should meet

$$T_i^A = n_i T^{\mathrm{LEO}}, n_i \ge 1, \forall i. \qquad (9)$$

In eq. (9), $n_i$ is a positive integer meeting $n_i \ge 1$. The ground station may transmit the wireless data once in every multiple orbital periods of the LEO satellite. Eq. (9) guarantees that the time of the wireless transmission at the ground station can always fall into its time window. Besides, by eq. (9), we have

$$T_i^W \le \min \left( T_i^A, \widetilde{T} \right) = \widetilde{T}.$$

because $T_i^A = n_i T^{\text{LEO}} \geq T^{\text{LEO}} > \widetilde{T}$.

In order to determine the $T_i^W$ ($0 \leq T_i^W \leq \widetilde{T}$) that maximizes the wireless transmission throughput, we introduce Lemma 2.

*Lemma 2:* The optimal $T_i^W$ that maximizes $R_i$ is $T_i^W = \widetilde{T}$.

*Proof:* When the energy of the ground stations is fixed, the transmission power consumption in the time $T_i^W$ is $P_i^W = \frac{E}{T_i^W}$. The corresponding amount of transmitted data can be expressed by

$$\mathsf{R}\left(P_i^W, T_i^W\right) = T_i^W B \log_2\left(1 + \frac{E|h_i|^2}{T_i^W \sigma^2}\right),$$

where $B$ is the wireless bandwidth. It can be proved that $\mathsf{R}(P_i^W, T_i^W)$ is increasing with $T_i^W$. This suggests that when $T_i^W = \widetilde{T}$, $\mathsf{R}(P_i^W, T_i^W)$ can be maximized.  ∎

From Lemma 2, we have $T_i^W = \widetilde{T}$. This derives that $\overline{P}_i^W = \frac{P_i^W \widetilde{T}}{T_i^A}$.

Next, we study the average power consumption of the computing server $\overline{P}_i^C$. Assume that the power of the computing server is $P_C$ W/cps. Then, the average power consumption of the computing server is $\overline{P}_i^C = \frac{P_C C_i T_i^C}{T_i^A}$. To further determine the variable $C_i$ in $\overline{P}_i^C$, we introduce Lemma 3.

*Lemma 3:* $\overline{P}_i^C = \frac{P_C w C_H}{T_i^A}$, and $C_i = \frac{\omega C_H}{T_i^A}$.

*Proof:* It can be proved that $\overline{P}_i^C = \frac{P_C C_i T_i^C}{T_i^A} = \frac{P_C w C_H}{T_i^A}$. Besides, the computing resource denoted by $C_i$ should be minimized to save system cost. According to (7), we have $C_i \geq \frac{\omega C_H}{T_i^A}$, which indicates that $C_i = \frac{\omega C_H}{T_i^A}$ is the minimal value of $C_i$.  ∎

In eq. (9), we first relax the integer variable $n_i$ to a continuous variable $\widetilde{n}_i$. After the optimization, the real number $\widetilde{n}_i$ can be dealt as the average number of $T^{\text{LEO}}$ for the satellite serving the ground station $i$. By the maximal average power constraint at each ground station $P_{\max}$, we can obtain the constraint (10) as

$$\overline{P}_i^S + \overline{P}_i^C + \overline{P}_i^W = 3K_i P_S + \frac{P_C \omega C_H}{\widetilde{n}_i T^{\text{LEO}}}$$

$$+ \frac{P_i^W \widetilde{T}}{\widetilde{n}_i T^{\text{LEO}}} \leq P_{\max}. \tag{10}$$

Besides, considering that the satellite can serve at most one ground station in each orbital period and $\widetilde{n}_i \geq 1$, we can obtain the following constraint:

$$\sum_{i=1}^{N} \frac{1}{\widetilde{n}_i} \leq 1. \tag{11}$$

Since the satellite can serve at most one ground station in each orbital period, $1/\widetilde{n}_i$ denotes the probability that the satellite serves for the ground station $i$ in an arbitrary orbital period of the satellite. By the constraints (10) and (11), the power allocation of caching, computing, and the communication can be integrated by the maximal available power $P_{\max}$.

## C. Nash Bargaining Game Based Terrestrial-Satellite System Model

In this paper, we formulate the system objective by the Nash bargaining game model. Let $\boldsymbol{\Omega}$ be a closed and convex subset denoting the set of feasible allocations that the players can obtain if they cooperate. We denote the utility function of the $i$-th player in game by $U_i$ ($1 \leq i \leq \widehat{N}$). Define $\boldsymbol{U}^{\min} = (U_1^{\min}, U_2^{\min}, \ldots, U_{\widehat{N}}^{\min})$ as the minimal gains of the $\widehat{N}$ players. Then, $(\boldsymbol{\Omega}, \boldsymbol{U}^{\min})$ constitutes the $\widehat{N}$-player Nash bargaining game. The key issue in Nash bargaining game is to find a Pareto efficient solution, from which no improvement for a subset of users can be attained without decreasing the utilities of other users. [11], [34]. Nash bargaining game has a unique fair Pareto optimal solution catering for the following axioms in Definition 1.

*Definition 1 ([11]):* Define $\mathbb{S}(\boldsymbol{\Omega}, \boldsymbol{U}^{\min})$ as the Nash bargaining game solution. Then, the properties of the Nash bargaining solution (NBS) $\boldsymbol{\phi} = \mathbb{S}(\boldsymbol{\Omega}, \boldsymbol{U}^{\min})$ are given by the following six axioms:

1) $\boldsymbol{\phi}$ is Pareto optimal.
2) Feasibility, i.e., $\boldsymbol{\phi} \in \boldsymbol{\Omega}$.
3) $\boldsymbol{\phi}$ guarantees the minimal utility $\boldsymbol{U}^{\min}$.
4) $\boldsymbol{\phi}$ guarantees the fairness by the independence of irrelevant alternatives. This indicates that if $\boldsymbol{\phi} \in \boldsymbol{\Omega}' \subset \boldsymbol{\Omega}$, and $\boldsymbol{\phi} = \mathbb{S}(\boldsymbol{\Omega}, \boldsymbol{U}^{\min})$, then $\boldsymbol{\phi} = \mathbb{S}(\boldsymbol{\Omega},' \boldsymbol{U}^{\min})$.
5) Independence of liner transformations. For a linear scale transformation $\hbar$, $\hbar(\mathbb{S}(\boldsymbol{\Omega}, \boldsymbol{U}^{\min})) = \mathbb{S}(\hbar(\boldsymbol{\Omega}), \hbar(\boldsymbol{U}^{\min}))$.
6) $\boldsymbol{\phi}$ guarantees the symmetry. Define the $i$-th player possesses the NBS $\phi_i$ in $\boldsymbol{\phi}$. If the $i$-th player and the $j$-th player have the same minimal utility in $\boldsymbol{U}^{\min}$, i.e., $\boldsymbol{U}_i^{\min} = \boldsymbol{U}_j^{\min}$, then, $\phi_i = \phi_j$. This effectively guarantees that all the players have the same priorities.

Axiom 5) indicates that the NBS is scale invariant. Axiom 6) suggests that the players with the same minimal demand of utility and the utility function will obtain the same utility. This guarantees fairness among the players. Hence, by Nash bargaining game, we can provide the ground stations with fair service.

Next, we design the system model maximizing Nash bargaining throughput in terrestrial-satellite system. We define $\xi_i = 1/\widetilde{n}_i$, where $\xi_i$ can be regarded as the time-sharing factor [11], *i.e.*, the proportion of time that the ground station $i$ occupies the time window of the satellite in an arbitrary orbital period. We also define $\widetilde{P}_i^W = \xi_i P_i^W$ leading to $P_i^W = \frac{\widetilde{P}_i^W}{\xi_i}$. Then, we can design the system objective as

$$\max_{\boldsymbol{\xi}, \boldsymbol{P}^W} \Upsilon = \sum_{i=1}^{N} \ln\left(\frac{\widetilde{T}}{T_i^A} R_i - R_i^{\min}\right)$$

$$= \sum_{i=1}^{N} \ln\left(\frac{\widetilde{T}\xi_i}{T^{\text{LEO}}} B \log_2\left(1 + \frac{\widetilde{P}_i^W |h_i|^2}{\xi_i \sigma^2}\right) - R_i^{\min}\right), \tag{12}$$

where $\boldsymbol{\xi} = \{\xi_i\}$, $\boldsymbol{P}^W = \{\widetilde{P}_i^W\}$, and $\{R_i^{\min}\}$ denotes the minimal required average throughput of the ground station $i$.

By $\widetilde{P}_i^W = \xi_i P_i^W$, we have

$$\overline{P}_i^W = \frac{P_i^W \xi_i \widetilde{T}}{T^{\text{LEO}}} = \frac{\widetilde{P}_i^W \widetilde{T}}{T^{\text{LEO}}}.$$

The constraints (10) and (11) can be re-written as follows,

$$\overline{P}_i^S + \overline{P}_i^C + \overline{P}_i^W$$
$$= 3K_i P_S + \frac{P_C \xi_i \omega C_H}{T^{\text{LEO}}} + \frac{\widetilde{P}_i^W \widetilde{T}}{T^{\text{LEO}}} \leq P_{\max}, \forall i. \quad \text{(C1)}$$

$$\sum_{i=1}^{N} \xi_i \leq 1. \quad \text{(C2)}$$

Eq. (C2) indicates that each orbital period of the satellite can serve at most one ground station. Since $\xi_i$ and $\widetilde{P}_i^W$ are nonnegative, we have

$$\xi_i \geq 0, \text{ and } \widetilde{P}_i^W \geq 0, \forall i. \quad \text{(C3)}$$

In eq. (C3), the ground station $i$ never transmits to the satellite if $\xi_i = 0$. Then, the system model can be formulated by

$$\max_{\boldsymbol{\xi}, \boldsymbol{P}^W} \Upsilon, \quad \text{(13a)}$$

$$\text{s.t. (C1), (C2) and (C3).} \quad \text{(13b)}$$

*Theorem 1:* The problem (13a) is a convex optimization problem.

*Proof:* It can be proved that the Hessian matrix of $\Upsilon$ in eq. (13a) over $\{\boldsymbol{\xi}, \boldsymbol{P}^W\}$ is negative semidefinite. This suggests that the objective in eq. (13a) is concave. Besides, we can also prove that the constraints (C1), (C2) and (C3) are all convex. Hence, problem (13a)–(13b) is a convex optimization problem. ∎

By Theorem 1, the utility in (13a) is concave and injective. Besides, all the intersection of the convex sets in (13a) is also a convex set. Then, it is proved that the proposed optimization model in (13a)–(13b) caters for the 6 axioms in Definition 1. Therefore, the proposed optimization model (13a)–(13b) meets Nash bargaining game theoretical architecture, and a unique Nash bargaining solution exists. Furthermore, we can employ dual decomposition to obtain the optimal solution.

## III. THE OPTIMAL RESOURCE ALLOCATION BY THE DUAL DECOMPOSITION

### A. Solution of the Nash Bargaining Based Optimization

In this section, we solve the optimization problem in (13a)–(13b) by dual decomposition method. Since the duality gap between the optimization model in eqs. (13a)–(13b) and its dual problem is zero, we can just solve the dual problem [11]. We define the Lagrange multiplier vectors $\mathcal{X} = \{\mathcal{X}_i\}$ and the Lagrange multiplier $\mathcal{Y}$. Obviously, the Lagrangian of the function in eqs. (13a)–(13b) can be formulated by eq. (14) shown at the bottom of this page. Moreover, in this paper, to solve eq. (14), we can first solve the inner layer problem in eq. (15) to obtain the resource allocation policy, and then solve the outer layer problem in eq. (15) to compute the dual variables iteratively,

$$\min_{\mathcal{X}, \mathcal{Y} \geq 0} \max_{\boldsymbol{\xi}, \boldsymbol{P}^W} \mathbb{L}\left(\boldsymbol{\xi}, \boldsymbol{P}^W, \mathcal{X}, \mathcal{Y}\right)$$
$$= \sum_{i=1}^{N} \mathcal{X}_i \left(P_{\max} - 3K_i P_S\right) + \mathcal{Y}$$
$$+ \Psi\left(\boldsymbol{\xi}, \boldsymbol{P}^W, \mathcal{X}, \mathcal{Y}\right), \quad \text{(15)}$$

where $\Psi(\boldsymbol{\xi}, \boldsymbol{P}^W, \mathcal{X}, \mathcal{Y})$ is formulated in eq. (16) shown at the bottom of this page. Then, given Lagrange multipliers, $\Psi(\boldsymbol{\xi}, \boldsymbol{P}^W, \mathcal{X}, \mathcal{Y})$ can be optimized by the Karush-Kuhn-Tucker (KKT) conditions. The optimal dual variables $\mathcal{X}$ and $\mathcal{Y}$ can be obtained by the ellipsolid and subgradient methods, etc.

We can obtain the optimal $\widetilde{P}_i^W$ for a specific ground station $i$ using the following result.

*Theorem 2:* The optimal power $\widetilde{P}_i^W$ for a specific ground station $i$ is

$$\widetilde{P}_i^W = \frac{\xi_i \sigma^2}{|h_i|^2} \left(\Gamma_i \exp\left(W\left(\ln 2^{\vartheta_i}\right)\right) - 1\right)^+,$$

where

$$\Gamma_i = 2^{\frac{R_i^{\min} T^{\text{LEO}}}{\widetilde{T} B \xi_i}},$$

$$\vartheta_i = \frac{|h_i|^2 T_i^{\text{LEO}}}{\ln 2 \xi_i \sigma^2 \mathcal{X}_i \widetilde{T} \Gamma_i},$$

$(x)^+ = \max(0, x)$, and $W(\cdot)$ denotes the Lambert-W function.

$$\mathbb{L}\left(\boldsymbol{\xi}, \boldsymbol{P}^W, \mathcal{X}, \mathcal{Y}\right) = \sum_{i=1}^{N} \ln\left(\frac{\widetilde{T} \xi_i}{T^{\text{LEO}}} B \log_2\left(1 + \frac{\widetilde{P}_i^W |h_i|^2}{\xi_i \sigma^2}\right) - R_i^{\min}\right)$$
$$+ \sum_{i=1}^{N} \mathcal{X}_i \left(P_{\max} - 3K_i P_S - \frac{P_C \xi_i \omega C_H}{T_i^{\text{LEO}}} - \frac{\widetilde{P}_i^W \widetilde{T}}{T^{\text{LEO}}}\right) + \mathcal{Y}\left(1 - \sum_{i=1}^{N} \xi_i\right) \quad \text{(14)}$$

$$\Psi\left(\boldsymbol{\xi}, \boldsymbol{P}^W, \mathcal{X}, \mathcal{Y}\right) = \sum_{i=1}^{N} \ln\left(\frac{\widetilde{T} \xi_i}{T^{\text{LEO}}} B \log_2\left(1 + \frac{\widetilde{P}_i^W |h_i|^2}{\xi_i \sigma^2}\right) - R_i^{\min}\right) - \sum_{i=1}^{N} \mathcal{X}_i \left(\frac{P_C \xi_i \omega C_H}{T^{\text{LEO}}} + \frac{\widetilde{P}_i^W \widetilde{T}}{T^{\text{LEO}}}\right) - \mathcal{Y} \sum_{i=1}^{N} \xi_i \quad \text{(16)}$$

*Proof:* We define $\varrho_i = 1 + \frac{\widetilde{P}_i^W |h_i|^2}{\xi_i \sigma^2}$. By the first derivative of $\Psi(\boldsymbol{\xi}, \boldsymbol{P}^W, \boldsymbol{\mathcal{X}}, \mathcal{Y})$ in eq. (16) with respect to $\widetilde{P}_i^W$, we have

$$\frac{\partial \Psi\left(\boldsymbol{\xi}, \boldsymbol{P}^W, \boldsymbol{\mathcal{X}}, \mathcal{Y}\right)}{\partial \widetilde{P}_i^W} = \frac{\frac{\widetilde{T}B}{T^{\mathrm{LEO}}} |h_i|^2}{\ln 2 \sigma^2}$$

$$\times \frac{\frac{1}{\varrho_i}}{\frac{\widetilde{T}B}{T^{\mathrm{LEO}}} \xi_i \log_2\left(\varrho_i\right) - R_i^{\min}} - \frac{\mathcal{X}_i \widetilde{T}}{T^{\mathrm{LEO}}} = 0.$$

Furthermore, we define $\Gamma_i = 2^{\frac{R_i^{\min} T^{\mathrm{LEO}}}{\widetilde{T}B \xi_i}}$. Then, we can derive that

$$\left(\frac{\varrho_i}{\Gamma_i}\right)^{\frac{\varrho_i}{\Gamma_i}} = 2^{\vartheta_i},$$

where

$$\vartheta_i = \frac{|h_i|^2 \widetilde{T}^{\mathrm{LEO}}}{\ln 2 \xi_i \sigma^2 \mathcal{X}_i \widetilde{T} \Gamma_i}.$$

By the Lambert-W function, $\frac{\varrho_i}{\Gamma_i}$ can be expressed by

$$\frac{\varrho_i}{\Gamma_i} = \exp\left(W\left(\ln 2^{\vartheta_i}\right)\right),$$

where $W(\cdot)$ denotes the Lambert-W function. Substituting $\varrho_i$ by $\varrho_i = 1 + \frac{\widetilde{P}_i^W |h_i|^2}{\xi_i \sigma^2}$, we have

$$\widetilde{P}_i^W = \frac{\xi_i \sigma^2}{|h_i|^2} \left(\Gamma_i \exp\left(W\left(\ln 2^{\vartheta_i}\right)\right) - 1\right)^+. \quad (17)$$

This proves Theorem 2. ∎

By Theorem 2, we can obtain the optimal power allocation $\widetilde{P}_i^W$. Likewise, by taking the first derivative of $\Psi(\boldsymbol{\xi}, \boldsymbol{P}^W, \boldsymbol{\mathcal{X}}, \mathcal{Y})$ with respect to $\xi_i$, we can obtain the optimal $\xi_i$ in Theorem 3.

*Theorem 3:* We define $\varsigma(\xi_i) = \frac{\partial \Upsilon}{\partial \xi_i}$. Then, $\varsigma(\xi_i)$ has its invertible function $\varsigma^{-1}(\cdot)$ when $R_i \geq R_i^{\min}$. The optimal $\xi_i$ is

$$\xi_i = \varsigma^{-1}\left(\mathcal{X}_i \frac{P_C w C_H}{T^{\mathrm{LEO}}} + \mathcal{Y}\right).$$

*Proof:* Define $\varsigma(\xi_i) = \frac{\partial \Upsilon}{\partial \xi_i}$, we can derive that

$$\varsigma(\xi_i) = \frac{\log_2\left(1 + \frac{\widetilde{P}_i^W |h_i|^2}{\xi_i \sigma^2}\right) - \frac{\widetilde{P}_i^W |h_i|^2}{\ln 2\left(\widetilde{P}_i^W |h_i|^2 + \xi_i \sigma^2\right)}}{\xi_i \log_2\left(1 + \frac{\widetilde{P}_i^W |h_i|^2}{\xi_i \sigma^2}\right) - \frac{R_i^{\min} T^{\mathrm{LEO}}}{\widetilde{T}B}}. \quad (18)$$

It can be proved that when

$$\frac{\xi_i \widetilde{T}B}{T^{\mathrm{LEO}}} \log_2\left(1 + \frac{\widetilde{P}_i^W |h_i|^2}{\xi_i \sigma^2}\right) > R_i^{\min},$$

$\varsigma(\xi_i) > 0$ and $\frac{\partial \varsigma(\xi_i)}{\partial \xi_i} < 0$. Hence $\varsigma(\xi_i)$ is strictly decreasing with $\xi_i$, and its invertible function $\varsigma^{-1}(\cdot)$ exists. By the first derivative of $\Psi(\boldsymbol{\xi}, \boldsymbol{P}^W, \boldsymbol{\mathcal{X}}, \mathcal{Y})$ in eq. (16) with respect to $\xi_i$, we have $\xi_i = \varsigma^{-1}(\mathcal{X}_i \frac{P_C w C_H}{T^{\mathrm{LEO}}} + \mathcal{Y})$. ∎

## B. Determine the Dual Variables

By eq. (15), the subgradient of $\mathcal{X}_i$ and $\mathcal{Y}$ can be represented by

$$\left(P_{\max} - 3K_i P_S - \frac{P_C \xi_i \omega C_H}{T^{\mathrm{LEO}}} - \frac{\widetilde{P}_i^W \widetilde{T}}{T^{\mathrm{LEO}}}\right),$$

and

$$\left(1 - \sum_{i=1}^N \xi_i\right),$$

respectively.

Given $\widetilde{P}_i^W$ and $\xi_i$ based on Theorem 2 and Theorem 3, the outer layer primal problem in eq. (15) can be solved by the gradient method. Then, the dual variables can be updated as follows:

$$\mathcal{X}_i(l+1) = \left(\mathcal{X}_i(l) - \ell_1(l)\left(P_{\max} - 3K_i P_S\right.\right.$$

$$\left.\left. - \frac{P_C \xi_i \omega C_H}{T^{\mathrm{LEO}}} - \frac{\widetilde{P}_i^W \widetilde{T}}{T^{\mathrm{LEO}}}\right)\right)^+, \quad \forall i, \quad (19)$$

$$\mathcal{Y}(l+1) = \left(\mathcal{Y}(l) - \ell_2(l)\left(1 - \sum_{i=1}^N \xi_i\right)\right)^+, \quad (20)$$

where $\ell_1(l)$ and $\ell_2(l)$ are the positive step size at the iteration $l$. Since the optimal objective (13a) is concave, the iteration can converge to the global optimal solution with an appropriate step size [11].

## C. The Algorithm Implementation

By Theorem 2, Theorem 3, and eqs. (19)–(20), we can obtain the global optimal $\{P_i^W\}$ and $\{\xi_i\}$ in an iterative manner. We propose the corresponding algorithm in Algorithm 1, called adaptive period of transmission (APT) algorithm.

By Algorithm 1, the satellite serving period and 3C power allocation can be optimized in an integrated process.

The convergence of the subgradient method based Algorithm 1 depends on the specific function, the number of variables, as well as the selection of step size, etc. In this paper, we can implement Algorithm 1 because that the number of variables is relatively small. More details about the computational complexity of subgradient method can be found in [38].

## IV. NUMERICAL RESULTS

In the simulation section, we set the noise temperature to be 260 K, and $R_i^{\min} = R_0/i$, $\forall i$, where $R_0$ is a constant given in Table I. We employ the path loss model

$$\mathfrak{L} = 92.44 + 20 \times \log_{10}(L) + 20 \times \log_{10}(f) \text{ dB},$$

where $f$ is the system operating frequency and $f = 2$ GHz. The unit of the distance $L$ is kilometer (km), and the unit of the frequency is GHz in the path loss model. We assume that $L = 100$ km. We consider the fast fading as complex Gaussian distribution $\mathcal{CN}(0, 1 \text{ dB})$, and the Shadow model as log-normal

TABLE I
SIMULATION PARAMETERS

| Parameter | Value |
|---|---|
| $N$ | 10 |
| $V$ | $5 \times \frac{\pi}{180}$ |
| $B$ | 50 MHz |
| $R_0$ | $2 \times 10^4$ bps |
| $P_{\max}$ | 50 dBW |
| $L$ | $10^5$ meter |
| $w$ | 1000 |
| $C_H$ | $10^{12}$ cycles |
| $P_c$ | $10^{-12}$ W/cps |
| $P_s$ | $10^{-15}$ W/bit |

---

**Algorithm 1:** Implementation of the APT Algorithm.

**Input:**
Initialize $l = 0$; initialize the sets of $\{\mathcal{X}_i(0)\}$ and $\mathcal{Y}(0)$;
initialize $\ell_1(0)$ and $\ell_2(0)$; initialize a very small constant
$\delta > 0$.
**Output:**
$\{P_i^W\}$ and $\{\xi_i\}$.
  **while** $|\widetilde{P}_i^W(l) - \widetilde{P}_i^W(l-1)| \le \delta$ and
  $|\xi_i(l) - \xi_i(l-1)| \le \delta$, $\forall i$ **do**
    **for** (each and all ground stations $i$) **do**
      Calculate $P_i^W(l)$ by Theorem 2;
      Calculate $\xi_i(l)$ by Theorem 3;
      Update $\mathcal{X}_i(l)$ by (19);
      Update $\mathcal{Y}(l)$ by (20);
      $l + 1 \rightarrow l$.
    **end for**
  **end while**
  $\xi_i(l) \rightarrow \xi_i$, $\forall i$.
  $\widetilde{P}_i^W(l) \rightarrow \widetilde{P}_i^W$ and $P_i^W = \frac{\widetilde{P}_i^W}{\xi_i}$, $\forall i$;

---

distribution $\mathcal{C}(0, 8\text{ dB})$. Unless otherwise specified, in the simulation section, the parameters are set as in Table I. In this paper, we compare the performance of the APT algorithm with that of the case $\xi_i = \frac{1}{N}$ ($\forall i$), called fixed period of transmission (FPT) algorithm. FPT algorithm corresponds to the case that the wireless transmission of the ground stations takes place in turn. By FPT algorithm, the ground stations occupy the satellite orbital period with an equal probability. Moreover, we call the APT with $R_i^{\min} = 0$, $\forall i$, as APTZ algorithm, and the FPT with $R_i^{\min} = 0$, $\forall i$, as FPTZ algorithm.

To measure the fairness of throughput among the ground stations, we use the Jains fairness metric formulated as follows.

$$
\mathcal{J} = \begin{cases} \dfrac{\left(\sum_{i=1}^N R_i\right)^2}{N \times \sum_{i=1}^N R_i^2}, & R_0 = 0, \\[18pt] \dfrac{\left(\sum_{i=1}^N \frac{R_i}{R_i^{\min}}\right)^2}{N \times \sum_{i=1}^N \left(\frac{R_i}{R_i^{\min}}\right)^2}, & R_0 \ne 0. \end{cases} \tag{21}
$$

In Fig. 5, we focus on the impact of $R_0$ on the system performance. In the simulation, when several ground stations cannot achieve its minimal throughput demand, the algorithm stops, and the throughput in this sample is zero. We re-run the simulation in multiple channel realizations and measure the average system performance in a long time. In Fig. 5(a), as $R_0$ increases, APTZ outperforms APT, and FPTZ outperforms FPT, respectively. This is because that increasing $R_0$ reduces the feasible solution space. As $R_0$ further increases, we find that the throughput of APT and FPT becomes zero, because a very large $R_0$ leads to infeasible 3C power allocation. Besides, from Fig. 5(a), we can observe that the APT based schemes can basically achieve larger throughput than that of the FPT based schemes. This confirms the effectiveness of the joint optimization of $\{P_i^W\}$ and $\{\xi_i\}$. In Fig. 5(b), the fairness among the ground station throughput is given. As $R_0$ increases, the fairness goes down because the probability that the ground stations not be served increases. In Fig. 5(c), we define $G = \frac{1}{N}\sum_{i=1}^N \tilde{n}_i$, and we give $G$ under different $R_0$. For APT and FPT, As $R_0$ increases, $G$ decreases, because the larger $R_0$ can increase the probability that the ground stations not be served in a long time. On the other hand, the increased $R_0$ leads to more frequent wireless transmission of the ground stations corresponding to the decreased $G$. Besides, $G = 10$ for the cases of APTZ and FPTZ when $R_0 = 0$, because $N = 10$ ground stations are assumed. However, when $R_0 \ne 0$, FPT possess $G < 10$, because the ground stations may not be served when the samples of the wireless channel quality is very poor, where $G = 0$ in this case.

In Fig. 6, we focus on the impact of $P_{\max}$ on the system performance. As in Table I, $R_0 = 2 \times 10^4$ bps for APT and FPT in Fig. 6. In Fig. 6(a), as $P_{\max}$ increases, the system throughput gradually increases. When $P_{\max}$ is large enough, the constraint on $R_0$ becomes inactive, where APT is equivalent to APRZ, and FPT is equivalent to FPRZ. This is because $R_0$ can be achieved when $P_{\max}$ is large enough. In Fig. 6(b), we can observe that the fairness of the ground stations gradually increases with $P_{\max}$ as well. This is because that the increased $P_{\max}$ can provide the ground stations with better service. In Fig. 6(c), as $P_{\max}$ increases, the performance gap of $G$ between APT and APTZ, as well as the performance gap of $G$ between FPT and FPTZ gradually narrows. This is because that the increased $P_{\max}$ can effectively weaken the impact of $R_0$ on the system performance. One interesting phenomenon in Fig. 6(c) is that unlike the cases of APT, FPT, and FPTZ, $G$ of APTZ gradually decreases as $P_{\max}$ increases. This is because that when $P_{\max}$ is relatively small, $G$ should be large enough to decrease the $\{\xi_i\}$ for meeting the power constraint in (C1). As $P_{\max}$ increases, $G$ in APTZ can be decreased to increase the corresponding $\{\xi_i\}$ for improving the system objective in eq. (13a). It is worth mentioning that when $P_{\max}$ is relatively small, $G$ of APT is smaller than the $G$ of APTZ because in several samples, the system cannot meet the constraint of $R_i^{\min}$ and stops working, where the average value of $G$ decreases. Likewise, when $P_{\max}$ is relatively small, $G$ of FPT is smaller than the $G$ of FPTZ. Besides, we can observe that in Fig. 6(b), unlike the cases of the throughput and $G$, the fairness performance gap between the APT and APTZ, as well as the gap between the FPT and FPTZ do not apparently decrease. This is because that the measurement of the fairness between the ground stations depends on whether $R_0 = 0$ as in eq. (21).
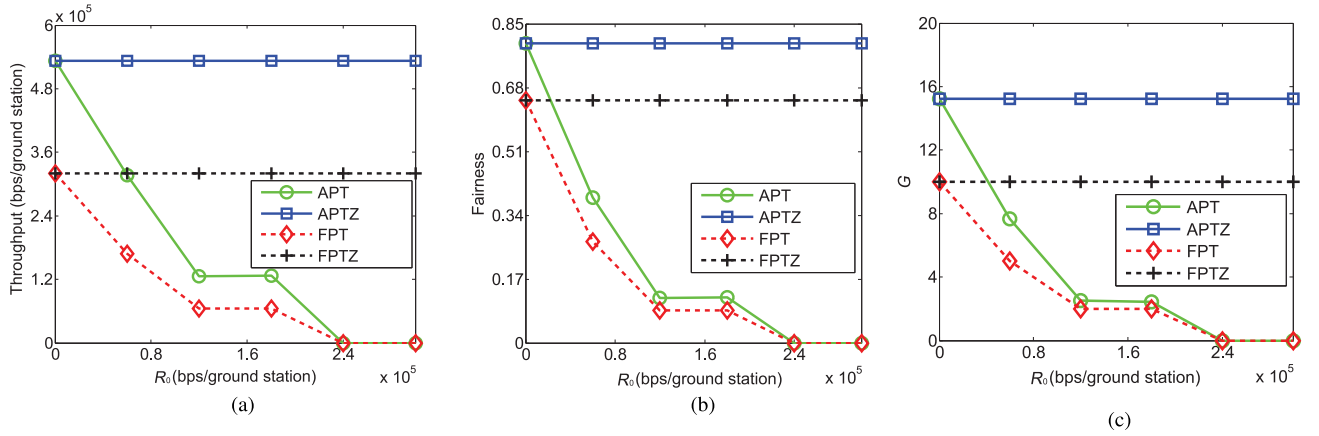
Fig. 5. The impact of $R_0$ on the system performance. (a) The impact of $R_0$ on the average throughput per ground station. (b) The impact of $R_0$ on the fairness of the ground stations. (c) The impact of $R_0$ on $G$.
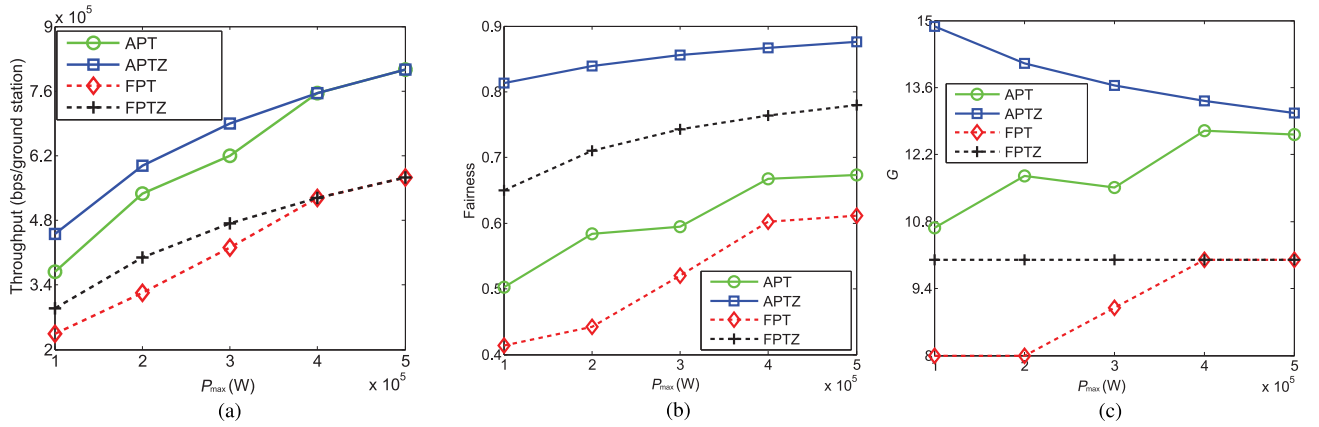


Fig. 6. The impact of $P_{\max}$ on system performance. (a) The impact of $P_{\max}$ on the average throughput per ground station. (b) The impact of $P_{\max}$ on the fairness of the ground stations. (c) The impact of $P_{\max}$ on the average number of circles of ground stations ($G$) transmitting one block to the satellites.
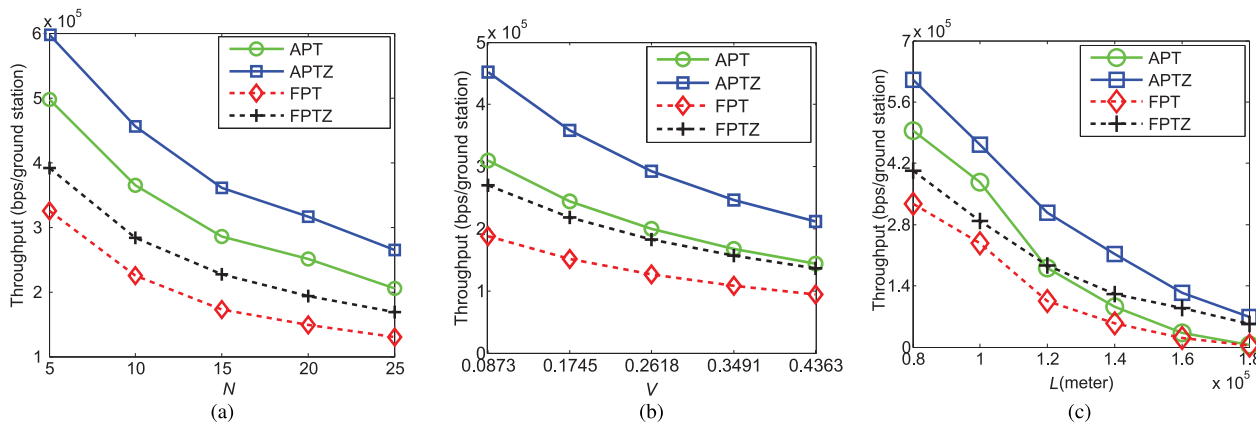


Fig. 7. The impact of $N$, $V$, and $L$ on the system throughput performance, respectively. (a) The impact of $N$ on the average throughput per ground station. (b) The impact of $V$ on the average throughput per ground station. (c) The impact of $L$ on the average throughput per ground station.

In Fig. 7, we further explore the throughput performance with the system parameters $N$, $V$, and $L$. In Fig. 7(a), as the number of ground stations $N$ increases, the throughput monotonously decreases. This is because that the increased $N$ may activate more ground stations with poor channel quality under the constraint on $R_i^{\min}$. In Fig. 7(b), the impact of the minimal elevation angle of the satellite to the ground stations $V$ on the system throughput performance is studied. As $V$ increases, the throughput performance monotonously decreases because a larger $V$ corresponds to a smaller $\widetilde{T}$. According to Lemma 2, less throughput will be obtain by the same transmitting power with a the smaller $\widetilde{T}$. In Fig. 7(c), as the distance between the satellite and the ground stations $L$ increases, the system throughput will monotonously decreases due to a larger path loss. Another observation in Fig. 7(c) is that the throughput performance of APT and FPT gradually approaches to each other as $L$ increases. The same phenomenon also exists in the throughput performance of APTZ and FPTZ. This is because as $L$ increases, the distance between the satellite and the ground stations dominates the channel gain, which makes $\{\xi_i\}$ equally for the ground stations. This indicates that the effectiveness of the adaptive adjusting $\{\xi_i\}$ gradually reduces as $L$ increases. The third observation in Fig. 7(c) is that as $L$ further increases, we find that FPTZ outperforms APT because by FPTZ, the satellites can serve the ground stations without the constraints of $R_i^{\min}$.

## V. CONCLUSION

In this paper, we have studied the joint optimization of satellite serving period and 3C power allocation in terrestrial-satellite systems considering user fairness and data security. Based on Nash bargaining, we improved the throughput of users while guaranteeing fairness. Besides, we also employed blockchain to guarantee data security. First, we divided system implementation into data accumulation, blockchain computing, and wireless transmission. Then, we revealed the relationship between the satellite serving period and the 3C power allocation through several theorems and lemmas. Last, we solved the Nash bargaining game based optimization problem with 3C power constraint using dual decomposition. Through extensive simulations, we have demonstrated the proposed optimal satellite serving period and the optimal 3C power allocation.
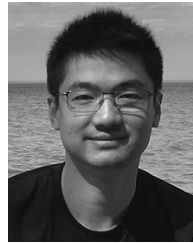
## REFERENCES

[1] N. Zhang, S. Zhang, P. Yang, O. Alhussein, W. Zhuang, and X. Shen, "Software defined space-air-ground integrated vehicular networks: Challenges and solutions," *IEEE Commun. Mag.*, vol. 55, no. 7, pp. 101–109, Jul. 2017.

[2] K. An, M. Lin, W. Zhu, Y. Huang, and G. Zheng, "Outage performance of cognitive hybrid satellite–terrestrial networks with interference constraint," *IEEE Trans. Veh. Technol.*, vol. 65, no. 11, pp. 9397–9404, Nov. 2016.

[3] C. Qiu, H. Yao, R. Yu, F. Xu, and C. Zhao, "Deep Q-learning aided networking, caching, and computing resources allocation in software-defined satellite-terrestrial networks," *IEEE Trans. Veh. Technol.*, vol. 68, no. 6, pp. 5871–5883, Jun. 2019.

[4] T. Zhang, H. Li, S. Zhang, J. Li, and H. Shen, "STAG-based QoS support routing strategy for multiple missions over the satellite networks," *IEEE Trans. Commun.*, vol. 67, no. 10, pp. 6912–6924, Oct. 2019.

[5] T. Zhang, H. Li, J. Li, S. Zhang, and H. Shen, "A dynamic combined flow algorithm for the two-commodity max-flow problem over delay-tolerant networks," *IEEE Trans. Wireless Commun.*, vol. 17, no. 12, pp. 7879–7893, Dec. 2018.

[6] G. Giambene, S. Kota, and P. Pillai, "Satellite-5G integration: A network perspective," *IEEE Netw.*, vol. 32, no. 5, pp. 25–31, Sep./Oct. 2018.

[7] X. Zhu, C. Jiang, L. Kuang, N. Ge, and J. Lu, "Non-orthogonal multiple access based integrated terrestrial-satellite networks," *IEEE J. Sel. Areas Commun.*, vol. 35, no. 10, pp. 2253–2267, Oct. 2017.

[8] X. Zhu, C. Jiang, L. Yin, L. Kuang, N. Ge, and J. Lu, "Cooperative multi-group multicast transmission in integrated terrestrial-satellite networks," *IEEE J. Sel. Areas Commun.*, vol. 36, no. 5, pp. 981–992, May 2018.

[9] J. Gao, S. A. Vorobyov, and H. Jiang, "Cooperative resource allocation games under spectral mask and total power constraints," *IEEE Trans. Signal Process.*, vol. 58, no. 8, pp. 4379–4395, Aug. 2010.

[10] Q. Ni and C. C. Zarakovitis, "Nash bargaining game theoretic scheduling for joint channel and power allocation in cognitive radio systems," *IEEE J. Sel. Areas Commun.*, vol. 30, no. 1, pp. 70–81, Jan. 2012.

[11] H. Zhang, C. Jiang, N. C. Beaulieu, X. Chu, X. Wang, and T. Q. S. Quek, "Resource allocation for cognitive small cell networks: A cooperative bargaining game theoretic approach," *IEEE Trans. Wireless Commun.*, vol. 14, no. 6, pp. 3481–3493, Jun. 2015.

[12] Z. Yang, K. Yang, L. Lei, K. Zheng, and V. C. M. Leung, "Blockchain-based decentralized trust management in vehicular networks," *IEEE Internet Things J.*, vol. 6, no. 2, pp. 1495–1505, Apr. 2019.

[13] M. Liu, F. R. Yu, Y. Teng, V. C. M. Leung, and M. Song, "Joint computation offloading and content caching for wireless blockchain networks," in *Proc. IEEE Conf. Comput. Commun. Workshops*, 2018, pp. 517–522.

[14] S. Fu, L. Zhao, X. Ling, and H. Zhang, "Maximizing the system energy efficiency in the blockchain based Internet of Things," in *Proc. IEEE Int. Conf. Commun.*, 2019, pp. 1–6.

[15] H. Liu, Y. Zhang, and T. Yang, "Blockchain-enabled security in electric vehicles cloud and edge computing," *IEEE Netw.*, vol. 32, no. 3, pp. 78–83, May/Jun. 2018.

[16] L. Zhou, L. Wang, Y. Sun, and P. Lv, "Beekeeper: A blockchain-based IoT system with secure storage and homomorphic computation," *IEEE Access*, vol. 6, pp. 43 472–43 488, 2018.

[17] H. Yin, D. Guo, K. Wang, Z. Jiang, Y. Lyu, and J. Xing, "Hyperconnected network: A decentralized trusted computing and networking paradigm," *IEEE Netw.*, vol. 32, no. 1, pp. 112–117, Jan./Feb. 2018.

[18] Y. Ren, C. Wang, Y. Chen, M. C. Chuah, and J. Yang, "Signature verification using critical segments for securing mobile transactions," *IEEE Trans. Mobile Comput.*, vol. 19, no. 3, pp. 724–739, Mar. 2020.

[19] C. Dai and Q. Song, "Heuristic computing methods for contact plan design in the spatial-node-based Internet of Everything," *IEEE China Commun.*, vol. 16, no. 3, pp. 53–68, Mar. 2019.

[20] S. Zhang, P. He, K. Suto, P. Yang, L. Zhao, and X. Shen, "Cooperative edge caching in user-centric clustered mobile networks," *IEEE Trans. Mobile Comput.*, vol. 17, no. 8, pp. 1791–1805, Aug. 2018.

[21] S. Fu, J. Wu, H. Wen, Y. Cai, and B. Wu, "Software defined wireline-wireless cross-networks: Framework, challenges, and prospects," *IEEE Commun. Mag.*, vol. 56, no. 8, pp. 145–151, Aug. 2018.

[22] A. K. Bairagi, N. H. Tran, W. Saad, Z. Han, and C. S. Hong, "A game-theoretic approach for fair coexistence between LTE-U and Wi-Fi systems," *IEEE Trans. Veh. Technol.*, vol. 68, no. 1, pp. 442–455, Jan. 2019.

[23] Q. Xu, Z. Su, and S. Guo, "A game theoretical incentive scheme for relay selection services in mobile social networks," *IEEE Trans. Veh. Technol.*, vol. 65, no. 8, pp. 6692–6702, Aug. 2016.

[24] F. Tschorsch and B. Scheuermann, "Bitcoin and beyond: A technical survey on decentralized digital currencies," *IEEE Commun. Surv. Tut.*, vol. 18, no. 3, pp. 2084–2123, Jul.–Sep. 2016.

[25] J. Liu, Y. Shi, L. Zhao, Y. Cao, W. Sun, and N. Kato, "Joint placement of controllers and gateways in SDN-enabled 5G-satellite integrated network," *IEEE J. Sel. Areas Commun.*, vol. 36, no. 2, pp. 221–232, Feb. 2018.

[26] J. Liu, Y. Shi, Z. M. Fadlullah, and N. Kato, "Space-air-ground integrated network: A survey," *IEEE Commun. Surv. Tut.*, vol. 20, no. 4, pp. 2714–2741, Oct.–Dec. 2018.

[27] N. Kato *et al.*, "Optimizing space-air-ground integrated networks by artificial intelligence," *IEEE Wireless Commun. Mag.*, vol. 26, no. 4, pp. 140–147, Aug. 2019.

[28] J. Gao, L. Zhao, and X. S. Shen, "Service offloading in terrestrial-satellite systems: User preference and network utility," in *Proc. IEEE Global Commun. Conf.*, 2019, pp. 1–6.

[29] J. Gao, L. Zhao, and X. Shen, "The study of dynamic caching via state transition field–the case of time-invariant popularity," *IEEE Trans. Wireless Commun.*, vol. 18, no. 12, pp. 5924–5937, Dec. 2019.

[30] J. Gao, L. Zhao, and X. Shen, "The study of dynamic caching via state transition field–the case of time-varying popularity," *IEEE Trans. Wireless Commun.*, vol. 18, no. 12, pp. 5938–5951, Dec. 2019.

[31] Z. Zhang, C.-H. Lung, I. Lambadaris, and M. St-Hilaire, "IoT data lifetime-based cooperative caching scheme for ICN-IoT networks," in *Proc. IEEE Int. Conf. Commun.*, 2018, pp. 1–7.

[32] J. Kwak, Y. Kim, L. B. Le, and S. Chong, "Hybrid content caching in 5G wireless networks: Cloud versus edge caching," *IEEE Trans. Wireless Commun.*, vol. 17, no. 5, pp. 3030–3045, May 2018.

[33] X. Sun and N. Ansari, "Dynamic resource caching in the IoT application layer for smart cities," *IEEE Internet Things J.*, vol. 5, no. 2, pp. 606–613, Apr. 2018.

[34] J. Gao, L. Zhao, and X. Shen, "Network utility maximization based on an incentive mechanism for truthful reporting of local information," *IEEE Trans. Veh. Technol.*, vol. 67, no. 8, pp. 7523–7537, Aug. 2018.

[35] M. S. Parwez and D. B. Rawat, "Resource allocation in adaptive virtualized wireless networks with mobile edge computing," in *Proc. IEEE Int. Conf. Commun.*, 2018, pp. 1–7.

[36] Q. Fan and N. Ansari, "Application aware workload allocation for edge computing-based IoT," *IEEE Internet Things J.*, vol. 5, no. 3, pp. 2146–2153, Jun. 2018.

[37] X. Chen, Q. Shi, L. Yang, and J. Xu, "Thriftyedge: Resource-efficient edge computing for intelligent IoT applications," *IEEE Netw.*, vol. 32, no. 1, pp. 61–65, Jan./Feb. 2018.

[38] S. Boyd and L. Vandenberghe, *Convex Optimization*. New York, NY, USA: Cambridge Univ. Press, 2004.

**Jie Gao** (Member, IEEE) received the B.Eng. degree in electronics and information engineering from the Huazhong University of Science and Technology, Wuhan, China, in 2007, and the M.Sc. and Ph.D. degrees in electrical engineering from the University of Alberta, Edmonton, AB, Canada, in 2009 and 2014, respectively. He is currently a Research Associate with the Department of Electrical and Computer Engineering, the University of Waterloo. He was a recipient of the Natural Science and Engineering Research Council of Canada Postdoctoral Fellowship, Ontario Centres of Excellence TalentEdge Fellowship, and Alberta Innovates-Technology futures graduate student scholarship. His research interests include the application of optimization, game theory and mechanism design, and machine learning in wireless communication networks and systems.

**Lian Zhao** (Senior Member, IEEE) received the Ph.D. degree from the University of Waterloo, Waterloo, ON, Canada, in 2002. She joined the Department of Electrical and Computer Engineering, Ryerson University, Toronto, Canada, in 2003 and was a Professor in 2014. Her research interests include the areas of wireless communications, radio resource management, mobile edge computing, caching and communications, and vehicular ad-hoc networks.

Dr. Zhao was selected as an IEEE Communication Society (ComSoc) Distinguished Lecturer for 2020 and 2021; received the Best Land Transportation Paper Award from the IEEE Vehicular Technology Society in 2016; Top 15 Editor in 2015 for IEEE TRANSACTION ON VEHICULAR TECHNOLOGY; Best Paper Award from the 2013 International Conference on Wireless Communications and Signal Processing and Best Student Paper Award (with her student) from Chinacom in 2011; the Canada Foundation for Innovation New Opportunity Research Award in 2005, and Early Tenure and promotion to Associate Professor in 2006. She is an Editor for IEEE TRANSACTIONS ON VEHICULAR TECHNOLOGY, IEEE TRANSACTIONS ON WIRELESS COMMUNICATIONS, IEEE *Internet of Things Journal*. She was Co-General Chair for the IEEE GreeenCom 2018; Co-Chair for the IEEE Globecom 2020 and IEEE ICC 2018 Wireless Communication Symposium; workshop Co-Chair for IEEE/CIC ICCC 2015; local arrangement Co-Chair for the IEEE Vehicular Technology Conference Fall 2017 and IEEE Infocom 2014; Co-Chair for IEEE Global Communications Conference 2013 Communication Theory Symposium. She was a Committee Member for Natural Science and Engineering Research Council of Canada, Discovery Grants Evaluation Group for Electrical and Computer Engineering 2015 to 2018; a Chair for the Professional Relations Committee for IEEE Canada for 2020. She is a licensed Professional Engineer in the Province of Ontario, a Senior Member of the IEEE Communication and Vehicular Society.

**Shu Fu** received the Ph.D. degree in communication and information system from the University of Electronic Science and Technology of China, Chengdu, China, in 2016. He is currently an Associate Professor with the College of Microelectronics and Communication Engineering, Chongqing University, Chongqing, China. His research interests include 5G network and terrestrial-satellite network, etc.